PERMAL: a machine learning approach for alpine permafrost distribution modeling

Nicola Deluigi and Christophe Lambiel

Institut de géographie et durabilité (IGD), Université de Lausanne, bâtiment Geopolis, CH-1015 Lausanne
nicola.deluigi@unil.ch, christophe.lambiel@unil.ch

Abstract

Most of the existing models of alpine permafrost distribution show a direct correlation between the permafrost occurrence and the increase in altitude. This may be correct at a regional scale, but it is often not valid at a more local scale, because of the high spatial discontinuity of alpine permafrost. For instance, the fact that permafrost is usually present only in the lower part of talus slopes has never been modeled. This paper presents a new model of alpine permafrost distribution that includes data obtained from field investigations carried out on various alpine landforms. The main goal of the study was to develop a model as reliable as possible at the local scale and to test the potential of an innovative approach in the field of permafrost modeling: Support Vector Machines (SVMs). This method is based on machine learning and provides a classification of samples produced by learning statistical dependencies between the studied phenomenon and other variables. This technique was used to model the spatial permafrost distribution in sedimentary landforms. In a second step, the lower limits of permafrost in rock walls, obtained by field measurements by PERMOS, were added to the model.

Keywords: mountain permafrost, modeling, machine learning, Support Vector Machines, *Swiss Alps*.

1 Introduction

Nowadays, permafrost mapping has a fundamental relevance for natural hazard prevention as for the design and the maintenance of infrastructures in high Alpine regions. As permafrost is invisible at the ground surface, its spatial modeling is one of the most important tasks of Alpine permafrost research. Initial efforts were proposed by HAEBERLI (1973) with the so-called empirical «rules of thumb», which considered the relationship between some topographic parameters and permafrost occurrence and were successively implemented in a GIS environment by KELLER (1992). Later, other spatial models were proposed by using rock glacier inventories (e.g. IMHOF 1996; DELALOYE and MORAND 1997; LAMBIEL and REYNARD 2001; BARONI *et al.* 2004; SEPPI *et al.* 2005), potential direct solar radiation (e.g. FUNK and HOELZLE 1992; HOELZLE and HAEBERLI 1995; FRAUENFELDER 1998; NYENHUIS *et al.* 2005), near ground surface and borehole temperatures (e.g. GRUBER *et al.* 2004; ETZELMÜLLER *et al.* 2006, 2007; ALLEN *et al.* 2009) or snow basal temperature (BTS) (e.g. KELLER *et al.* 1998; GRUBER and HOELZLE 2001; EBOHON and SCHROTT 2008). These models generally offer a good overview of the potential spatial distribution of mountain permafrost at the regional scale. Other more process oriented models (e.g. STOCKER-MITTAZ *et al.* 2002) succeeded to simulate with good accuracy the ground temperature at the point scale, but the high number of input parameters needed prevent a regionalization of the information. All in all, there is a lack of models able to simulate the strong heterogeneity of mountain permafrost at the local scale (e.g. LAMBIEL and PIERACCI 2008; SCAPOZZA and LAMBIEL, this volume). The majority of existing models indicate a general correlation between permafrost occurrence and the increase of altitude (KELLER 1992; IMHOF 1996; GRUBER and HOELZLE 2001; BAFU 2005; BOECKLI *et al.* 2012). If

this may appear correct at a regional scale, it is not always valid at a more local scale, because of the high spatial discontinuity of the permafrost extension. Effectively, recent studies have shown that Alpine permafrost is usually present only in the lower half of talus slopes in relation to the so-called chimney effect, allowing air circulation through coarse blocky surfaces (DELALOYE et al. 2003a; MORARD et al. 2010; SCAPOZZA et al. 2011).

The first goal of this study is to propose a new model aiming at integrating and simulating the heterogeneity of mountain permafrost, and thus to propose a model as reliable as possible at the local scale. Accordingly, a machine learning approach was adopted (cf. 3.1). Thus, the second objective of the study is to test the potential of this innovative approach in the field of permafrost modeling.

2   Study area and known permafrost distribution

For this study, we choose the entire Swisstopo 1:25 000 "Rosablanche" topographic map to develop and to test the model. The research area is located in the Western Swiss Alps and it covers three main valleys: Bagnes, Nendaz and Hérémence. Since 1998, the Mont Gelé – Mont Fort region, situated in the western part of the map (Verbier/Nendaz area), has been studied by several field campaigns conducted by the geography institutes of the universities of Lausanne and Fribourg. The first attempts to estimate the potential permafrost distribution were proposed by REYNARD (1996), REYNARD et al. (1999), and LAMBIEL and REYNARD (2001, 2003), thanks to geomorphological mapping, rock glacier inventoring and 1-D resistivity prospecting. During the last decade, various methods such as electrical resistivity tomography, seismic refraction, ground (surface) temperature measurements and borehole logging were used to map the permafrost distribution and to characterize the ground stratigraphy in different landforms such as rock glaciers, talus slopes and moraine deposits (e.g. TURATTI 2002; DELALOYE et al. 2003b; REYNARD et al. 2003; MARESCOT et al. 2003; DELALOYE 2004; DELALOYE and LAMBIEL 2005; LAMBIEL 2006; LAMBIEL and PIERACCI 2008; LAMBIEL and SCHUETZ 2008; HILBICH 2009; SCAPOZZA et al. 2011; SCAPOZZA 2012).

As we will describe in the next chapter, the modeling approach chosen for this study requires a calibration based on examples that indicate the permafrost occurrence. The availability of data for the Mont Gelé-Mont Fort region made the Rosablanche topographic map the best choice for this purpose.

3   Methodical background

3.1   Learning from data

The last decades were characterized by the development of numerical models based on physical or statistical approaches. The relevance of these tools, as help for decision-making, became crucial since the availability of a wide number of spatial data and measurements, which have increased due to technological improvements in automated environmental monitoring. Rapidly, the research field of statistical machine learning grew, permitting the analysis of huge volumes of data and to discovery of the dependencies hidden inside them (KANEVSKI et al. 2009). The application of the binary classification to machine learning was one of most important tasks introduced by the Statistical Learning Theory (VAPNIK 1998). Without, a priori, any users' assumptions about phenomena distribution, data-driven algorithms should search for a decision function discriminating all samples of a dataset in two binary classes (such as "absence" or "presence" of a phenomenon). The classification is produced by learning statistical dependencies between the studied phenomenon and other variables in a so-called training samples dataset. These techniques should supply to

accurate decision boundaries, taking into account non-linear solutions and misclassifications of observed data samples.

For this study, a technique providing these requirements and considering the complexity of the permafrost distribution was necessary. This complexity is linked to a high amount of variables (predictors), which lead to a high dimensional feature space of factors related to the permafrost occurrence. Therefore, Support Vectors Machines (SVMs) were chosen because of their suitability for high-dimensional datasets, avoiding model overfitting and allowing a probabilistic interpretation of the outputs through a continuous decision function. However, this method requires abundant examples that indicate the presence of permafrost. Since a good set of training samples indicating the permafrost distribution was unavailable for rock walls, SVMs were only used to predict the permafrost distribution in sedimentary landforms such as rock glaciers and talus slopes. The lower limits of permafrost in rock walls were obtained by field measurements from the Swiss Permafrost Monitoring Network (PERMOS 2009) (Fig. 1) and added to the model in a second step.
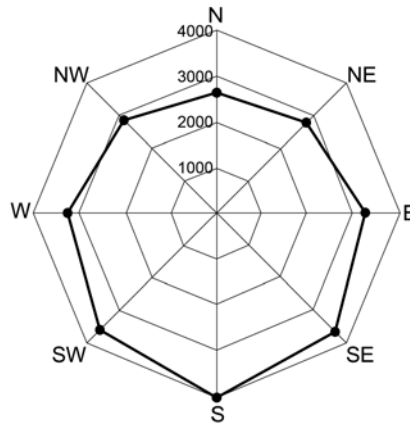

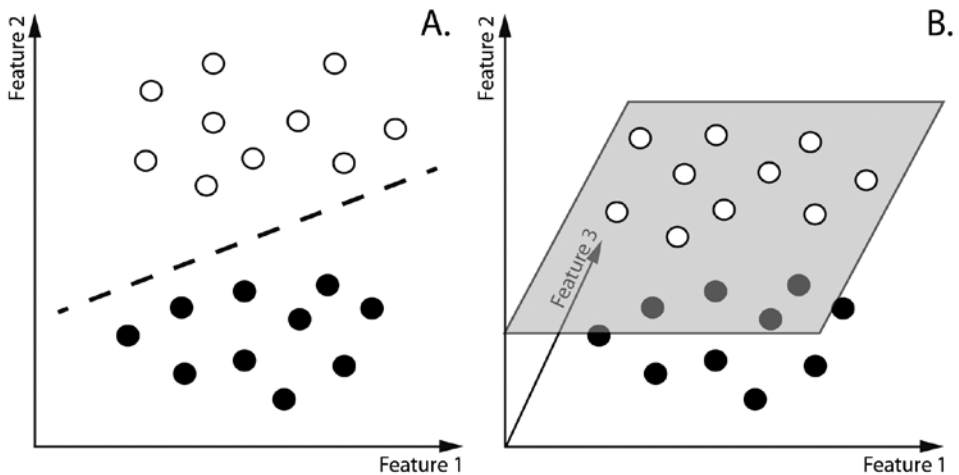Fig. 1. permafrost lower limits in rockwalls, resulting from PERMOS (2009) field measurements.

Fig. 2. linear separable samples in 2-D (A) and 3-D (B) features space.

3.2   Support Vector Machines

3.2.1   Main concepts

The main concept of SVMs introduced by VAPNIK (1998) indicates that, when dealing with a problem in which different objects have to be divided in two categories by placing a discriminating boundary, the most intuitive option is to draw a separating line. In an N-dimensional space, the line becomes a hyperplane (Fig. 2).

With a SVMs approach, we must firstly suppose that the data samples $(x_1, y_1), \ldots, (x_N, y_N)$, where x are the input features (e.g. see Table 1) and $y \in \{-1; +1\}$ the binary labels (e.g. absence and presence of permafrost), are linearly separable. This allows samples to be classified into two binary classes. The SVMs algorithm aims to determine the function that maximizes the distance between the training points and the hyperplane (the so-called margin ρ). The linear decision function is defined as

$$f(x) = wx + b \tag{1}$$

where w is a weighing vector which needs to be optimized along with the scalar b in order to maximize the margin ρ. The maximal margin is obtained by minimizing $\frac{1}{2}\|w\|^2$. Moreover, the sign of the function $f(x)$ determines the class in which a predicted sample belongs. The optimization of the parameters w and b is a quadratic programming problem with linear constraints and unique solution. Furthermore, w is defined as a linear combination of the training samples x_i, in which almost the total of them have a weight α_i equal to zero:

$$w = \sum_{i=1}^{N} \alpha_i y_i x_i \tag{2}$$

The solution of the optimization problem allows the SVMs decision function to be formulated as

$$f(x) = \sum_{i=1}^{N} \alpha_i y_i x x_i + b \tag{3}$$

All nearest samples to the decision boundary are the only ones that contribute to the maximum margin solution. They have a non-zero weight and they are called Support Vectors (Fig. 3).

A linearly separable data samples case, where the two classes are not overlapping, is an ideal situation one will rarely be dealing with. In fact, data could be noisy and it is not always possible to avoid training errors when drawing a separating line. The SVMs classifier accounts for overlapping data with a soft margin adaptation: slack variables ξ_i are assigned to noisy samples lying outside their class margin. Therefore, at this point, a coefficient that affects the trade-off between complexity and proportion of non-separable samples is required and it must be selected by the user (CHERKASSKY and MULIER 1998). For this reason, a so-called cost hyper-parameter C is added to the optimization in order to keep a balance between empirical error and the minimization of $\frac{1}{2}\|w\|^2$ for the finding of the largest possible margin ρ.

Up to this point, we have seen how a linear decision function can be optimally applied in order to classify our examples with binary labels. When dealing with datasets where the input/output relationships are non-linear (Fig. 4A), we need to find a more clever way to discriminate the two classes. The tricky idea is to map the dataset into a space of higher

dimensions and then to perform the well-known linear separation on the transformed data (Fig. 4B), rather than applying complex decision functions directly on the initial dataset. In this case, a "kernel trick" is used in equation (3) to substitute the dot product between the input vector of a sample x and all training samples x_i with a kernel function $K(\cdot,\cdot)$, allowing non-linear decision boundaries to be determined. Accordingly, the final formulation of the decision function for a classification task takes the form:

$$f(x) = \sum_{i=1}^{N} \alpha_i y_i K(x, x_i) + b \qquad (4)$$

Among the available kernel functions, a user's choice often falls on the Gaussian Radial Basis Function (Gaussian RBF) kernel $e^{-\frac{(x-x_i)^2}{2\sigma^2}}$ because of the simple geometrical interpretation it provides. The parameter σ, controlling the bandwidth of the Gaussian surface centered on vector x, needs to be tuned using a validation dataset.
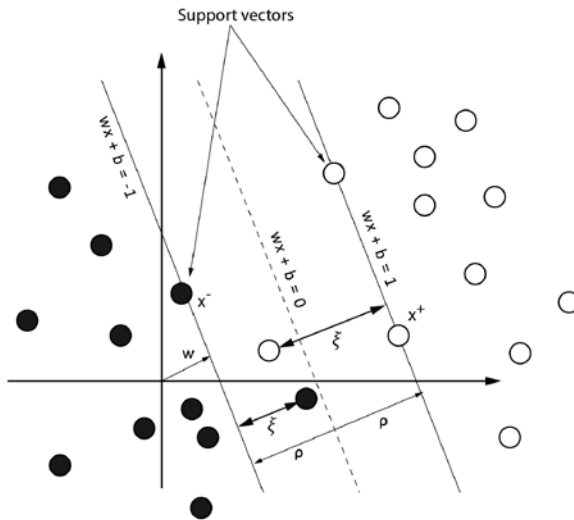

Fig. 3. binary classification of two groups of samples by maximizing the margin ρ and allowing misclassifications.
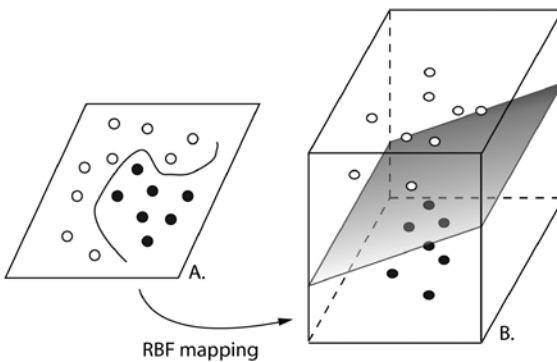

Fig. 4. RBF mapping allowing non-linear classification in a linear space to be solved.

3.2.2   Data preparation

For this case study a pool of 15 features was retained (Table 1). Some variables are strictly related to permafrost presence or absence, but for some of them a generalization was necessary. This was, for example, the case for glacier forefields, in which permafrost is often restricted to the lateral and frontal margin (e.g. REYNARD *et al.* 2003). For simplicity, we decided to label this variable as an indicator of permafrost absence.

Altitude, potential direct solar radiation, aspect, slope and curvature were simply extrapolated from the Swisstopo's digital elevation model with a 25×25 meter resolution. Lakes, human infrastructures, current glacier extension and mineral/vegetation-covered surfaces were extracted from the Swisstopo's primary surfaces map. From these variables, other features were calculated. The mean annual air temperature (MAAT) was obtained for the entire Rosablanche map with a linear regression involving daily temperatures measured at Les Attelas ENET meteorological station, according to BOUËT's (1985) formulas. Moreover, glacier forefields were extrapolated by subtracting the current glacier extension from the Little Ice Age glacier extension (MAISCH 1999). Talus slopes and rock wall mapping was produced by a DEM-based geomorphometric approach proposed by LOYE *et al.* (2009), which permitted the identification of these features according to a slope angle distribution analysis. Intact rock glaciers (actives and inactives) were extracted from the region's rock glacier inventory (LAMBIEL 1999; LAMBIEL and REYNARD 2003). The dataset was completed by empirical data from field campaigns, which show permafrost presence in talus slopes.

Table 1. the list of features used for the permafrost distribution modeling in sedimentary landforms.

Variable	Permafrost occurrence	Description
Altitude	–	Elevation in meters
Aspect	–	Exposition in degrees
Slope	–	Slope angle in degrees
Potential direct solar radiation	–	Direct solar radiation for the snow-free period (1st July-31 October)
MAAT	–	Mean annual air temperature (in degrees) for the 1996-2009 period
Curvature	–	Topographic curvature in degrees
Glacier	Unlikely/Rare	Binary variable indicating glacier presence/absence ('1' or '0')
Intact rock glacier	Probable	Binary variable indicating rock glacier presence/absence ('1' or '0')
Human infrastructure	Unlikely	Binary variable indicating human infrastructure presence/absence ('1' or '0')
Lake	Unlikely	Binary variable indicating lake presence/absence ('1' or '0')
Glacier forefield	Unlikely/Rare	Binary variable indicating glacier forefield presence/absence ('1' or '0')
Mineral-covered surface	Possible	Binary variable indicating mineral-covered surface presence/absence ('1' or '0')
Rock wall	Possible	Binary variable indicating rock wall presence/absence ('1' or '0')
Vegetation	Unlikely	Binary variable indicating vegetation presence/absence ('1' or '0')
Talus slope	Possible	Binary variable indicating talus slope presence/absence ('1' or '0')

The input vectors were composed of several groups of features for each location. In order to reduce the dimensionality, all values were standardized (z-score). The goal of the SVMs training process was to generate discriminative predictants related to permafrost occurrence (presence, absence or uncertainty). On a total of 295 680 samples (pixels), 6193 of them indicated presence of permafrost (2 %) and 182 173 indicated absence of permafrost (62 %). The last 107 314 samples (36 %) were unlabelled and needed to be classified (Fig. 5). Only a small portion of samples were randomly extracted from the two first categories and used for the training process. This means that SVMs predicted the permafrost occurrence for the entire study area. Remaining samples from these categories were used to validate the model. In fact, the modeling process involved a random partitioning of the original dataset into 3 sub-datasets: a training set to fit the model and maximize margins, a validation set to estimate the prediction error for model selection (tuning hyperparameters) and a test set, used for assessment of the generalization error of the final chosen model. This process was repeated 30 times using different random sample pools and different proportions between the sub-datasets.

3.2.3   Prediction process and probabilistic SVMs output interpretation for decision support and model accuracy

By using the training set to find the final decision function, the classification was possible. The so-called prediction process was then executed, in which each unlabelled pixel was placed under or above the margin ρ (hyperplane). During this simulation phase, the test sets were also used to validate the final model and to calculate its error.

In the Statistical Learning Theory, VAPNIK (1998) shows that the SVMs approach usually provides an excellent generalization ability and accurate predictions in high dimensional spaces. Moreover, this technique usually avoids over-fitting and accounts auto-correlation
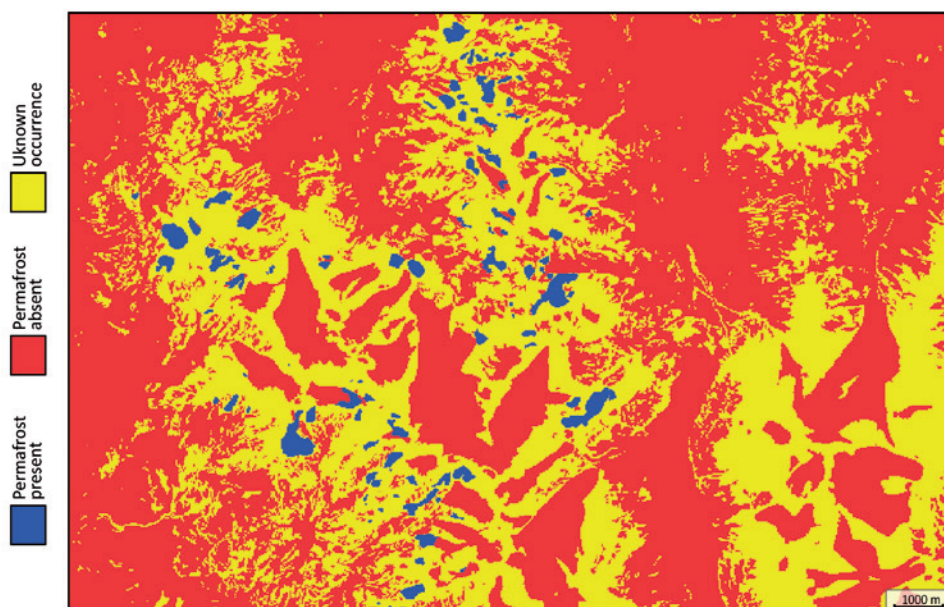

Fig. 5. labeled samples (pixels) used by Support Vector Machines (SVMs) for the simulation.

between similar input features. However, decision function output labels $y = \{-1; +1\}$ are difficult to interpret and employ for decision making. A smooth confident measure $p: 0 < p(y = \{-1; +1\}|x) < 1$ is computable by using the PLATT (1999) sigmoid function:

$$p = \frac{1}{1+\exp{(A \cdot f(x)+B)}} \tag{5}$$

where A and B are the parameters to tune on the validation set in order to avoid model over-fitting.

To evaluate the quality of this modeling, two approaches were chosen: the overall accuracy ratio (OAR) (6) and the area under the receiver-operating characteristics (AUROC). The first ratio, which ranges between 0 and 1, reports the number of correct predictions over the total number of points, indicating the reliability of the model. The receiver-operating characteristic (ROC) plots in a 2-dimensional graph the false positive rate (horizontal axis) (7) and the true positive rate (the vertical axes) (8). It results in an interesting quality measure because a SVMs binary classification is executed according to a defined threshold resulting in a positive class label if the score is above the threshold t ($f(x) > t$), or in a negative one if the value is lower than t ($f(x) < t$). When computing these TP/FP rates for the classifications obtained with thresholds varying from their minimal to maximal values, we will be able to plot a point (FP rate, TP rate) associated with each selected threshold (FAWCETT 2006; HAMEL 2009). AUROC ranges between 0.5, which means a random model behavior, and 1 (perfect model).

$$Overall\ accuracy\ ratio = \frac{hits+correct\ negatives}{total} \tag{6}$$

$$False\ positive\ rate = \frac{false\ alarms}{falses\ alarms+correct\ negatives} \tag{7}$$

$$True\ positive\ rate = \frac{hits}{hits+misses} \tag{8}$$

The final model was evaluated with the means of all OAR and AUROC calculated for each of the 30 sub-sets.

4   Results and discussion

4.1   The Rosablanche permafrost extension map

The SVMs final model indicates all values calculated by the decision function (Fig. 6). Values ($f(x) < -1$ or $f(x) > +1$ or $f(x) > +1$) correspond to samples that are labeled as a negative or a positive class, or more precisely as a pixel in which permafrost is absent or present. However, all values predicted in the $[-1; +1]$ range (between margins) cannot be classified with certitude. The Platt sigmoid function (5) is then required in order to allow a probabilistic interpretation of these samples.

Resulting occurrence probabilities (Fig. 7) were classified into three categories. Predictions below 0.4 were classified as "permafrost absent". The remaining 0.6 was divided into two equal classes: from 0.4 to 0.7 predictions were labeled as "permafrost possible"; from 0.7 to 1.0 as "permafrost probable". Figure 8 illustrates the final model of the potential permafrost extent, called PERMAL (for "Permafrost Machine Learning"), which was produced by merging the probabilistic SVMs output with the permafrost map for rock walls resulting from PERMOS (2009) measured lower limits.
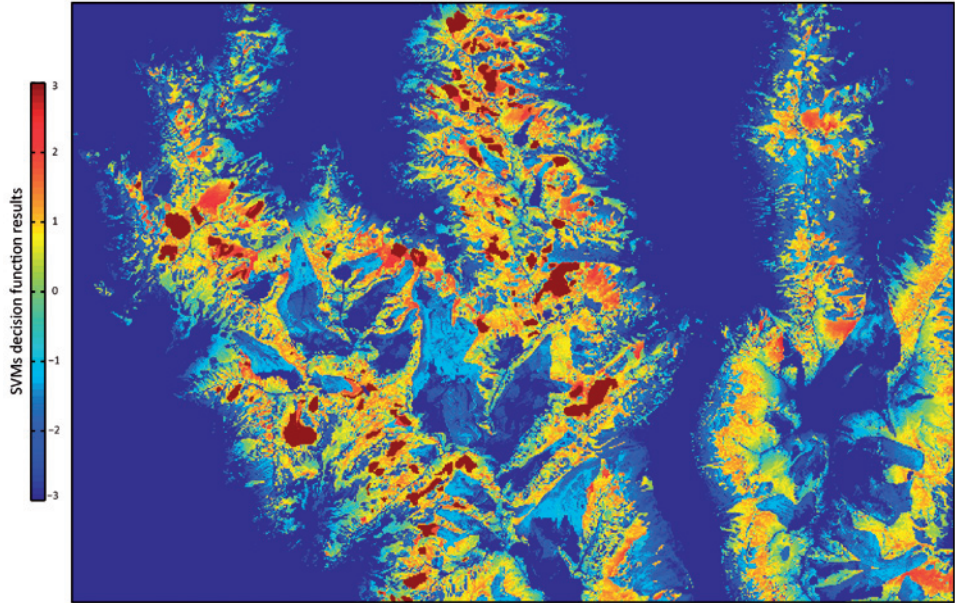
Fig. 6. Support Vector Machines decision function results. Pixel values require a probabilistic transformation to be interpreted (see 3.2.3).
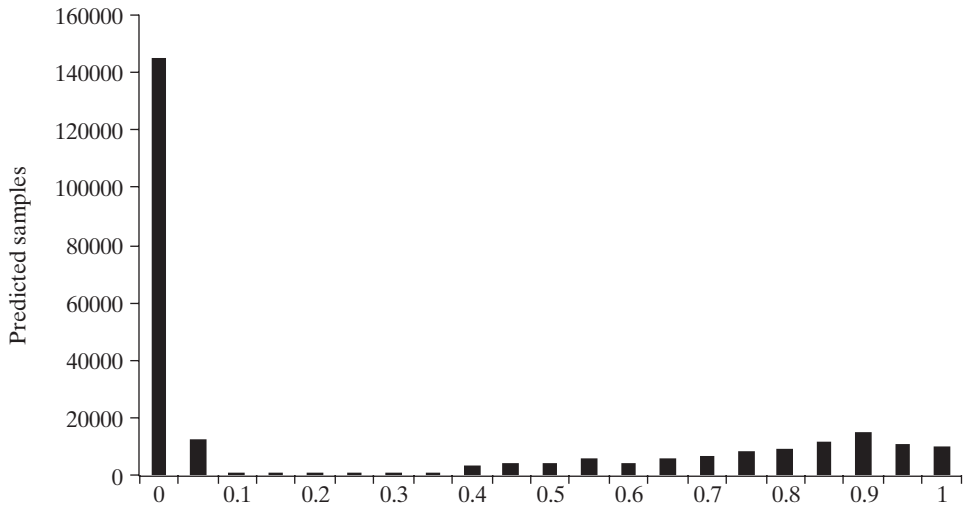

Fig. 7. distribution of permafrost occurrence's probabilities resulting from the Platt sigmoid function (see 3.2.3).
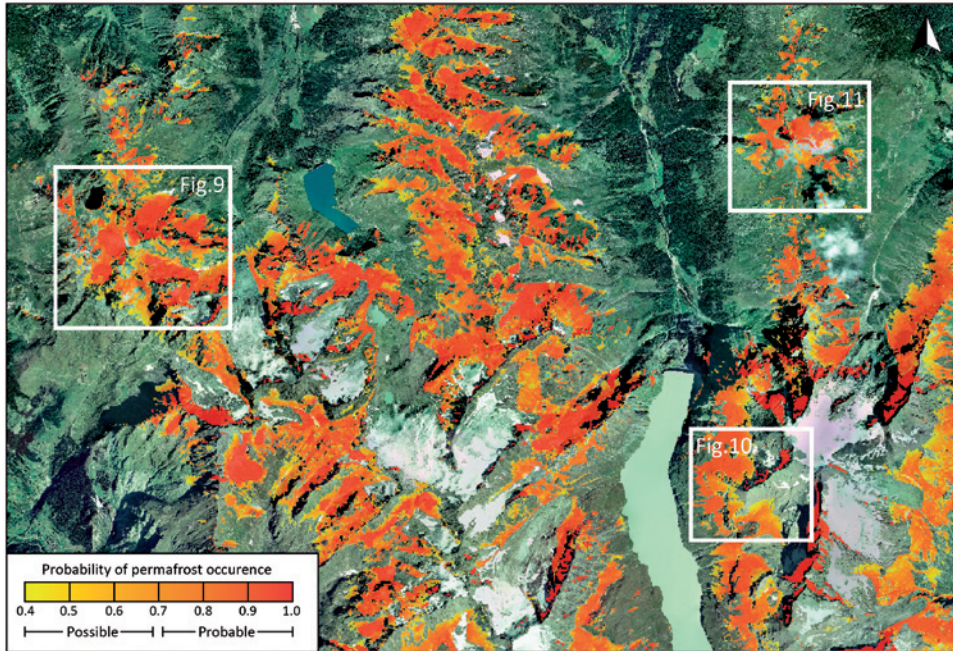
Fig. 8. the final potential alpine permafrost distribution map for the entire Rosablanche topographic map area.

4.2   PERMAL result analysis

In order to provide a quantitative analysis, the OAR and the AUROC were calculated, providing values of 0.967, respectively 0.975. These rates indicate an almost perfect model, which is usually synonym of a model over-estimation. Unluckily, SVMs are a "black-box" type modeling, a disadvantage the machine learning methods are often criticized for. This means that it is impossible to understand in what way predictors influenced the permafrost occurrence without the embedding of additional algorithms. As a result, we must suppose that the permafrost extent is probably less important than the modeled one.

A qualitative analysis was carried out on selected regions of interest. The Mont Gelé sector (Fig. 9A) provides good examples of how SVMs predicted the permafrost occurrence for different landforms. Training samples, such as rock glaciers of the Yettes Condja valley (a), periglacial lobes at Lac des Vaux (b) and the Lapires talus slope (c) were correctly recognized. On the other hand the decrease of permafrost occurrence with altitude in the talus slopes was not modeled correctly (c, d). Another result is that permafrost boundaries were automatically limited to mineral-covered surfaces, according to the Swisstopo's primary surfaces mapping (e).

Darbonneire and Tsauderys glacier circuses (Fig. 10A) supply supplementary examples that illustrate the way SVMs modeled the permafrost extension. These sectors are characterized by extended mineral-covered surfaces and are particularly interesting because they do not contain any training samples. For the entire area, the permafrost distribution was simulated by the SVMs calculated decision function. The PERMAL result appears correct for all eights aspects. Northern exposed slopes are characterized by a more important permafrost occurrence than the south-facing ones. Furthermore, permafrost was predicted as absent for
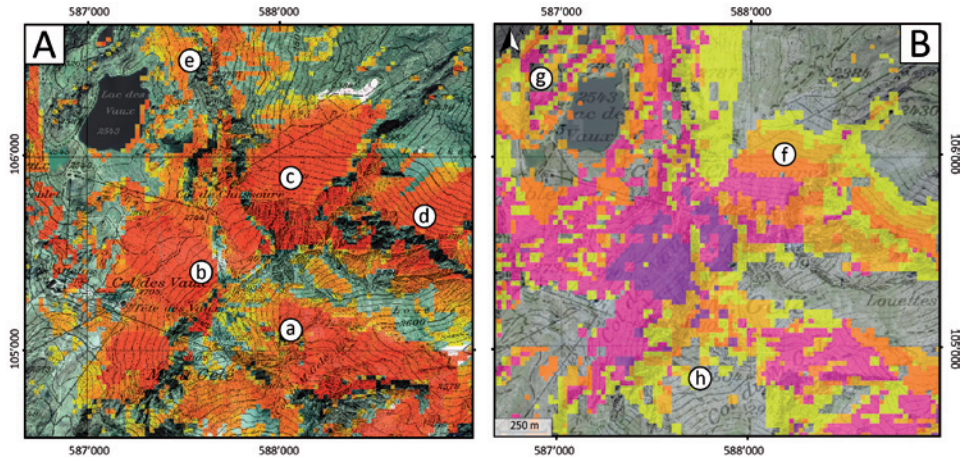
Fig. 9. PERMAL simulation (A) versus the BAFU one (B) for the Mont Gelé sector. Refer to text for the meaning of the small letters.
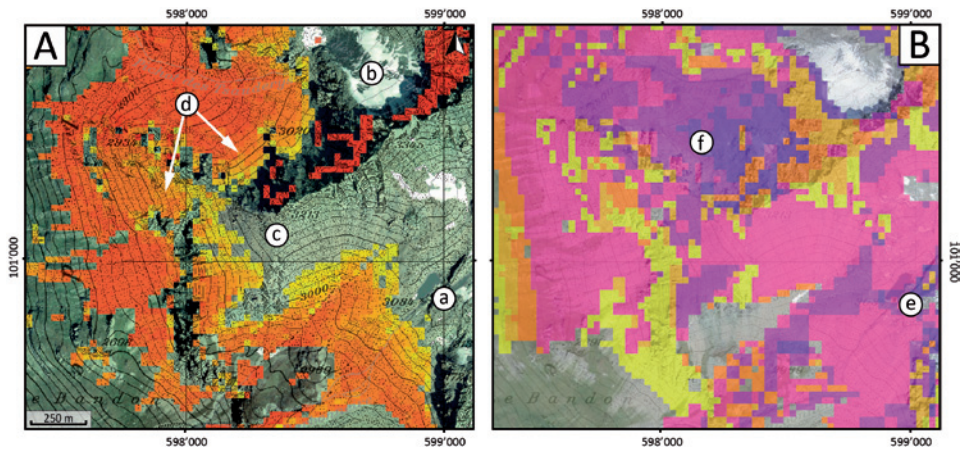

Fig. 10. PERMAL simulation (A) versus the BAFU one (B) for the Darbonneire and Tsauderys glacier circuses sector. Refer to text for the meaning of the small letters.

the Darbonneire glacier forefield (a) and for the Tsauderys glacier surface (b). For most talus slopes, permafrost occurrence was simulated as probable. However, some contrasts can be observed between the lower and the upper parts of some slopes. It is especially the case in the center of the map (c), where PERMAL predicted a total absence of permafrost for the upper part of these regular slopes. In sector d, even though the lower part was not clearly separated from the upper part of the slope, a decrease in the probability of permafrost occurrence with altitude was modeled. Thus, for these sectors, SVMs appears to be modeling correctly the atypical permafrost distribution for talus slopes.

The last example illustrates the permafrost distribution for the Pic d'Artisinol area (Fig. 11A and 12). PERMAL simulated correctly a low occurrence of permafrost in vegetation-covered slopes and probabilities above 40% for mineral-covered surfaces. The two rock

glaciers located on the Northeastern side of the Pic d'Artsinol (b) were not provided to the machine because they were not included in the rock glacier inventory used for the training process. As indicated in figure 12, SVMs were capable of predicting the boundaries of these landforms with accuracy.
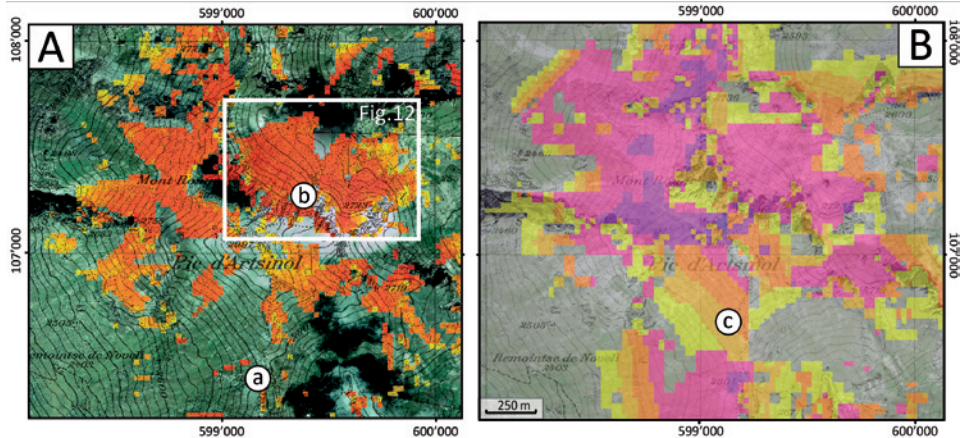

Fig. 11. PERMAL simulation (A) versus the BAFU one (B) for the Pic d'Artsinol sector. For the significance of the small letters see the text. The highlighted zone corresponds to the zoom in Fig. 12.
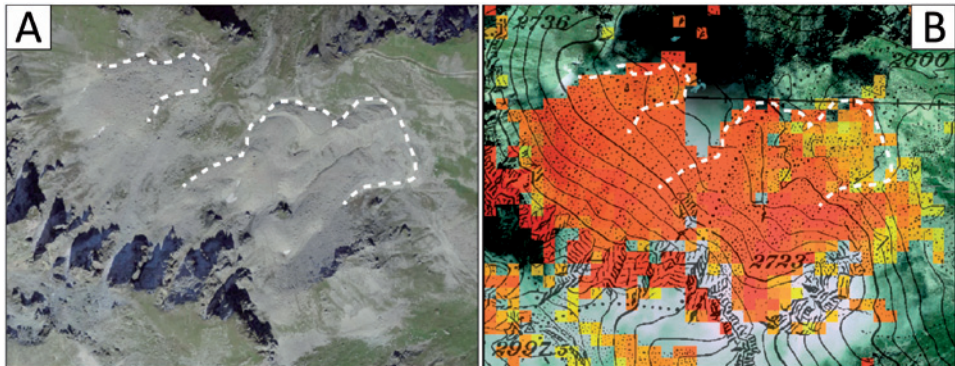

Fig. 12. Rock glacier limits (A) and PERMAL simulation (B) in the northern part of the Pic d'Artsinol.

4.3   PERMAL – BAFU comparison

In order to show the PERMAL qualities and limitations, a comparison with the BAFU model is proposed. In this model, two different approaches were used for sedimentary landforms and for bedrock. The modeling of permafrost in sediment was based on the "rules of thumb" of Haeberli (1973) and implemented in the PERMAKART model by Keller (1992), For bedrock, the modeling was based on a physical model developed by Gruber *et al.* (2004). In the end, the BAFU map is built from different altitude thresholds above which permafrost may be found.

For the Mont Gelé sector (Fig. 9), PERMAL and the BAFU model show quite different results. For example, in the Lapires talus slope, the BAFU map shows a direct correlation between permafrost occurrence and the increase of altitude (f), contrary to PERMAL, which presents the same probability for the entire slope. Despite the fact that the contrast between the upper part and the lower part has not been modeled by PERMAL, this result is nevertheless more in accordance with the field data (Scapozza 2012). Moreover, PERMAL considers the boundaries between vegetation and mineral-covered surfaces in a better way then the BAFU model. On the one hand, this provides an extension map in which permafrost is not present in vegetation-covered surfaces, as for slopes around the Lac des Vaux (g). On the other hand, PERMAL sometimes indicates doubtful permafrost presence for sites characterized by mineral cover. The south-facing slope of the Mont Gelé (h) is a good example in which we observe that the BAFU map, because of altitude thresholds, does not show any permafrost occurrence, contrary to PERMAL that simulates permafrost presence, probably because it recognizes a mineral-covered slope.

For both Darbonneire-Tsauderys glaciers circuses and Pic d'Artsinol sectors (Fig. 10, 11 and 12), the BAFU model is more optimistic and the permafrost extension is more important than what PERMAL simulates. It's interesting to observe that samples labeled as "permafrost probable" are almost the same for both models. Nevertheless, some important differences need to be evoked. For the first site, the BAFU model points out permafrost presence in the Darbonneire's glacier forefield (e). Also, contrary to PERMAL, this model does not consider a lower permafrost probability for the upper half of talus slopes (f). This sector clearly illustrates the consequence of the altitude thresholds used by the BAFU model for the permafrost simulation: gradually as the altitude increases, the permafrost probability becomes higher. In a similar way, these thresholds are evidently shown in the Pic d'Artsinol area (Fig. 11). South of the summit, different bands of probability are simulated and their altitudes vary according to the aspect of the slope (c). Moreover, for this site, we observe that the BAFU model predicts permafrost presence also for vegetation-covered slopes, which is generally not the case with PERMAL (a).

5   Conclusion

PERMAL appears to be thorough in the simulation of the high discontinuity of mountain permafrost. Results revealed a rather good reliability with the field data and a good discrimination between mineral and vegetation surfaces, where permafrost is often absent. An important advantage of PERMAL is that it does not use any altitude thresholds, conversely to the BAFU model. In the end, comparisons between both models showed that PERMAL is less optimistic than the BAFU model. Presented examples indicate that results of PERMAL may be more consistent with the field data than those of the BAFU model.

Nevertheless, the presented analysis indicated some limitations. Firstly, the "black-box" model characterization of SVMs does not allow the weights of the variables and their importance for the permafrost occurrence to be understood. These predictors were chosen in accordance to field data and consecutively included in the dataset. However, more variables could be added. For example, in order to improve the results and to better model the contrast of permafrost occurrence between the lower and the upper part of talus slopes, two new predictors should be included in the dataset ("lower part" and "upper part" of the slope). These discriminating variables could help SVMs to recognize the pixel localization in the slope. Thus, a more significant occurrence of permafrost in the lower part of the slopes could be simulated. In fact, this contrast was modeled only for a couple of examples. Besides, boundaries that describe vegetation and mineral-covered surfaces are precisely taken into account by PERMAL. Accordingly, Swisstopo's primary surfaces must be accurate to obtain a reliable result. Thus, next improvements should include more accurate data extracted from

satellite and aerial images, and high resolution DEMs. Further development would also require more detailed information about grain size of mineral-covered surfaces, in order to predict a higher permafrost occurrence in coarse blocky slopes and to better simulate the strong heterogeneity of mountain permafrost at the local scale.

6   References

ALLEN, S.; GRUBER, S.; OWENS, I., 2009: Exploring steep bedrock permafrost and its relationship with recent slope failures in the Southern Alps of New Zealand. Permafrost Periglacial Process. 20: 345–356.

BARONI, C.; CARTON, A.; SEPPI, R., 2004: Distribution and behaviour of rock glaciers in the Adamello-Presanella massif (Italian Alps). Permafrost Periglacial Process. 15: 243–259.

BOECKLI, L.; BRENNING, A.; GRUBER, S.; NOETZLI J., 2012: A statistical permafrost distribution model for the European Alps. Cryosphere 6: 125–140.

BOUËT, M., 1985: Climat et météorologie de la Suisse romande. Lausanne, Payot (2nd edition).

Bundesamt für Umwelt (BAFU), 2005: Hinweiskarte der potenziellen Permafrostverbreitung der Schweiz.

CHERKASSKY, V.; MULIER, F., 1998: Learning from Data: Concepts, Theory, and Methods. New York, Wiley. 441 p.

DELALOYE, R., 2004: Contribution à l'étude du pergélisol de montagne en zone marginale. Fribourg, département des Géosciences. GeoFocus No. 10.

DELALOYE, R.; LAMBIEL, C., 2005: Evidence of winter ascending air circulation throughout talus slopes and rock glaciers situated in the lower belt of alpine discontinuous permafrost (Swiss Alps). Norsk Geografisk Tifsskrift 59, 2: 194–203.

DELALOYE, R.; MORAND, S., 1997: Du Val Ferret au Grand-Combin (Alpes valaisannes): inventaire des glaciers rocheux et analyse spatiale du pergélisol à l'aide d'un système d'information géographique (IDRISI). Travail de Diplôme, Institut de Géographie de l' Université de Fribourg [unpublished].

DELALOYE, R.; REYNARD, E.; LAMBIEL, C.; MARESCOT, L.; MONNET, R., 2003a: Thermal anomaly in a cold scree slope (Creux du Van, Switzerland). 8th International Permafrost Conference, Zurich, Switzerland. 175–180.

DELALOYE, R.; LAMBIEL, C.; REYNARD, E.; LUGON, R., 2003b. Réponse du pergélisol à l'avancée glaciaire du Petit Age Glaciaire: quelques exemples alpines et pyrénéens. Environnements périglaciaires, Bull. de l'Ass. Fr. Périglaciaire 10.

EBOHON, B.; SCHROTT, L., 2008: Modeling Mountain Permafrost Distribution: a new map of Austria. 9th International Conference on Permafrost, Fairbanks, Alaska. 25: 397–402.

ETZELMÜLLER, B.; HEGGEM, E.; SHARKHUU, N.; FRAUENFELDER, R.; KÄÄB, A.; GOULDEN, C., 2006: Mountain permafrost distribution modelling using a multi-criteria approach in the Hövsgöl area, Northern Mongolia. Permafrost Periglacial Process. 17: 91–104.

ETZELMÜLLER, B.; FARBROT, H.; GUDHMUNDSSON, A.; HUMLUM, O.; TVEITO, O.; BJÖRNSSON, H., 2007: The regional distribution of mountain permafrost in Iceland. Permafrost Periglacial Process. 18: 185–199.

FAWCETT, T., 2006: An introduction to roc analysis. Pattern Recognit. Lett. 27: 861–874.

FRAUENFELDER R., 1998: Permafrostuntersuchungen mit GIS. Eine Studie im Fletschhorngebiet. Mitt. Vers.anst. Wasserbau Hydrol. Glaziol. Eidgenöss. Tech. Hochsch. Zür. 158: 55–68.

FUNK, M.; HOELZLE, M., 1992: A model of potential direct solar radiation for investigating occurrences of mountain permafrost. Permafrost Periglacial Process: 3, 139–142.

GRUBER, S.; HOELZLE, M., 2001: Statistical modelling of mountain permafrost distribution: local calibration and incorporation of remotely sensed data. Permafrost Periglacial Process. 12, 1: 69–77.

Gruber, S.; King, L.; Kohl, T.; Herz, T.; Haeberli, W.; Hoelzle, M., 2004: Interpretation of geothermal profiles perturbed by topography: the Alpine permafrost boreholes at Stockhorn Plateau, Switzerland. Permafrost Periglacial Process. 15, 4: 349–357.

Haeberli, W., 1973: Die Basis-Temperatur der winterlichen Schneedecke als möglicher Indikator für die Verbreitung von Permafrost in den Alpen. Z. Gletsch.kd. Glazialgeol. IX,1/2: 221–227.

Hamel, L., 2009: Model assessment with roc curves. Department of Computer Science and Statistics. University of Rhode Island, USA.

Hilbich C., 2009: Geophysical monitoring systems to assess and quantify ground ice evolution in mountain permafrost. PhD thesis, Friedrich Schiller University of Jena. 173 pp.

Hoelzle, M.; Haeberli, W., 1995: Simulating the effects of mean annual air temperature changes on permafrost distribution and glacier size. An example from the Upper Engadin, Swiss Alps. Ann. Glaciol. 21: 400–405.

Kanevski, M.; Pozdnoukhov, A.; Timonin, V., 2009: Machine Learning for Spatial Environmental Data. Lausanne, EPFL Press.

Keller, F.,1992: Automated Mapping of Mountain Permafrost Using the Program PERMAKART within the Geographical Information System ARC/INFO. Permafrost Periglacial Process. 3: 133–138.

Keller, F.; Frauenfelder, R.; Hoelzle, M.; Kneisel, C.; Lugon, R.; Phillips, M.; Reynard, E.; Wenker, L., 1998: Permafrost map of Switzerland. Proceedings of the 7th International Conference on Permafrost, Nordicana, Yellowknife, Canada. 557–562.

Imhof, M., 1996: PERM-ein Programm für die automatisierte Kartierung von Permafrost in den Schweizer Alpen. In: Haeberli, W.; Hoelzle, M.; Dousse, J.-P.; Ehrler, C.; Gardaz, J.-M.; Imhof, M.; Keller, F.; Kunz, P.; Lugon, R.; Reynard, E. (eds) Simulation der Permafrostverbreitung in den Alpen mit geographischen Informationssystemen. Arbeitsbericht NFP 31, Zürich, Hochschulverlag AG an der ETHZ. 25–33.

Lambiel, C.,1999: Inventaire des glaciers rocheux entre le Val de Bagnes et le Val d'Hérémence (Valais). Mémoire de licence, Institut de Géographie, Université de Lausanne, [unpublished].

Lambiel, C.; Reynard, E., 2001: Regional modelling of present, past and future potential distribution of discontinuous permafrost based on a rock glacier inventory in the Bagnes-Hérémence area (Western Swiss Alps). Norsk Geografisk Tidsskrift 55: 219–223.

Lambiel, C.; Reynard, E., 2003: Cartographie de la distribution du pergélisol et datation des glaciers rocheux dans la région du Mont Gelé (Valais). Entwicklungstendenzen und Zukunftsperspektiven in der Geomorphologie. Phys. Geogr. 41: 91–104.

Lambiel, C., 2006: Le pergélisol dans les terrains sédimentaires à forte déclivité: distribution, régime thermique et instabilités. Lausanne, Institut de Géographie. Trav. rech. 33.

Lambiel, C. ; Pieracci, K., 2008: Permafrost distribution in talus slopes located within the alpine periglacial belt, Swiss Alps. Permafrost Periglacial Process. 19, 3: 293–304.

Lambiel, C.; Schuetz, P., 2008: Ground characteristics and deformation of a frozen moraine affected by tourist infrastructures (Col des Gentianes, Valais). Klimaveränderungen auf der Spur. Studien des Europäischen Tourismus Instituts an der Academia Engiadina, Samedan, 5, 110–122.

Loye, A.; Jaboyedoff, M.; Pedrazzini, A., 2009: Identification of potential rockfall source areas at a regional scale using a DEM-based geomorphometric analysis. Nat. Hazards Earth Syst. Sci. 9: 1643–1653.

Maisch, M.,1999: Die Gletscher der Schweizer Alpen – Gletscherhochstand 1850, aktuelle Vergletscherung, Gletscherschwund-Szenarien (NFP31 final report). Zürich, vdf Hochschulverlag. 376 pp.

Marescot, L.; Loke, M.; Chapellier, D.; Delaloye, R.; Lambiel, C.; Reynard, E., 2003: Assessing reliability of 2D electrical resistivity imaging in mountain permafrost studies using the depth of investigation index method. Near Surf. Geophys. 1: 57–67.

Morard, S.; Delaloye, R.; Lambiel, C., 2010: Pluriannual thermal behaviour of low elevation cold talus slopes in western Switzerland. Geogr. Helv. 65, 2: 124–134.

Nyenhuis, M.; Hoelzle, M.; Dikau, R., 2005: Rock glacier mapping and permafrost distribution modelling in the Turtmanntal, Valais, Switzerland. Z. Geomorphol. 49: 275–292.

Platt, J., 1999: Probabilist Outputs for Support Vector Machines and Comparisons to Regularized Likelihood Method: Advances in Large Margin Classifiers, MIT Press.

PERMOS, 2009: Permafrost in Switzerland 2004/2005 and 2005/2006. In: Noetzli, J.; Naegeli, B.; Vonder Muehll, D. (eds) Glaciological Report (Permafrost) No. 6/7 of the Cryospheric Commission of the Swiss Academy of Sciences. 100 pp.

Reynard, E., 1996: Glaciers rocheux et limite inférieure du pergélisol discontinu dans le vallon de Tortin (Valais). Bull. Murithienne 114.

Reynard, E.; Delaloye, R.; Lambiel, C., 1999: Prospection géoélectrique du pergélisol alpin dans le massif des Diablerets (VD) et au Mont Gelé (Nendaz, VS). Bull. Murithienne 117: 89–103.

Reynard, E.; Lambiel, C.; Delaloye, R.; Devaud, G.; Baron, L.; Chapellier, D.; Marescot, L.; Monnet, R., 2003: Glacier/permafrost relationships in forefields of small glaciers (Swiss Alps). 8th International Permafrost Conference, Zurich, Switzerland. 947–952.

Scapozza, C.; Lambiel, C.; Baron, L.; Marescot L.; Reynard, E., 2011: Internal structure and permafrost distribution in two alpine periglacial talus slopes, Valais, Swiss Alps. Geomorphol. 132: 208–221.

Scapozza, C., 2012: Stratigraphie, morphodynamique, paléoenvironnements des terrains sédimentaires meubles à forte déclivité du domaine périglaciaire alpin. Thèse de Doctorat, Université de Lausanne, Géovisions 41: 551 pp.

Scapozza, C.; Lambiel, C., 2013: Structure interne et dynamique de fluage de l'éboulis "à galets" de Tsaté-Moiry (VS). In: Graf, C. (Red.) Mattertal – ein Tal in Bewegung. Publikation zur Jahrestagung der Schweizerischen Geomorphologischen Gesellschaft 29. Juni – 1. Juli 2011, St. Niklaus. Birmensdorf, Eidg. Forschungsanstalt WSL. 33–45.

Seppi, R.; Carton, A.; Baroni, C., 2005: Proposta di una nuova scheda per il censimento dei rock glaciers da fotografie aeree: applicazione sull'Alta Val Ultimo (Gruppo Ortles-Cevedale). Geogr. Fis. Dinam. Quat. 7: 329–338.

Stocker-Mittaz, C.; Hoelzle, M.; Haeberli, W., 2002: Permafrost distribution modeling based on energy-balance data: a first step. Permafrost Periglacial Process. 13, 4: 271–282.

Turatti, A., 2002: La discontinuité du pergélisol dans l'éboulis des Lapires (Nendaz/VS). Travail de diplôme. Dep. Geosciences, Univ. Fribourg [unpublished].

Vapnik, V., 1998: Statistical Learning Theory. New York, Wiley. 736 p.